JOURNAL OF MATERIALS SCIENCE 20 (1985) 3649–3660

Hysteresis effects on the high-temperature internal friction of polycrystalline zirconium

F. POVOLO
Comisión Nacional de Energía Atomica, Dto. de Materiales, Av. del Libertador 8250, (1429) Buenos Aires, Argentina

B. J. MOLINAS
Instituto de Física Rosario (CONICET-UNR), Facultad de Ciencias Exactas e Ingeniería, Universidad Nacional de Rosario, Av. Pellegrini 250, (2000) Rosario, Argentina

Hysteresis effects present on the high temperature internal friction of annealed polycrystalline zirconium are investigated in detail. It is shown that two internal friction maxima are present when the measurements are performed on heating. If a high enough temperature is reached, only one internal friction maxima is observed on cooling. Furthermore, when the temperature is not decreased below a certain value (critical temperature) only the lower temperature peak is present during a subsequent heating cycle. The critical temperature is strongly dependent on the grain size. Finally, both the hysteresis effects and the internal friction maxima are explained by relaxation mechanisms associated with grain boundary sliding and segregation of impurities to the grain boundaries.

1. Introduction

The presence of grain boundaries in metals and alloys has been known to produce internal friction peaks on the high temperature internal friction (HTIF) since the earliest work by Kê [1]. Most experimental results on grain boundary damping in pure metals and alloys have been reviewed by Gleiter and Chalmers [2]. An orthodox or low temperature peak is observed in pure metals, which is generally attributed to a grain boundary sliding mechanism since the height of the peak decreases as the grains grow to sizes comparable to the cross-section of the specimens. Addition of impurities reduces the height of the original grain boundary peak and simultaneously a new "solute peak" occurs, generally at higher temperatures. This peak is attributed to a segregation of impurities to grain boundaries.

The models based on grain boundary sliding, used to explain the HTIF maxima, have been criticized mainly based on two arguments:

1. the grain boundary peak is found to be amplitude dependent [3–8];

2. relaxation effects are present in slightly deformed single crystals in the same temperature range as the grain boundary peak [5–14].

Based on these arguments several authors concluded that the grain boundary peaks must be explained by mechanisms which are not specific to the grain boundary itself, but involve more generally the climb and glide of lattice dislocations. Some of the weak points of these lattice dislocation models, however, have been recently pointed out by Kê [15]. Furthermore, in our opinion the evidence presented to demonstrate the amplitude dependence of the grain boundary peak is not clear. In fact, the internal friction curves as a function of temperature, obtained at different strain levels, show that the strain amplitude affects mainly the internal friction background and not the grain boundary peak [3–8].

In the particular case of zirconium and

0022–2461/85 $03.00 + .12

zirconium alloys, Ritchie and Sprungmann [7, 8] have studied the amplitude and temperature dependence of the HTIF of α-zirconium single and polycrystals. The damping spectra were resolved into five peaks: one peak due to the thermally assisted unpinning of dislocations, two peaks associated with longitudinal and transverse redistribution of oxygen interstitials on dislocations, a peak associated with special dislocation structures and a grain boundary peak. Also a background was observed that increased exponentially with temperature. it must be pointed out, however, that Ritchie and Sprungmann observed generally only one maximum, above about 673 K, on the HTIF of zirconium, with location and shape strongly dependent on the thermomechanical treatment given to the specimens. Sometimes, a second maximum, also observed by Gacougnolle and coworkers [16–18], could be partially resolved from the HTIF. The five internal friction peaks reported by Ritchie and Sprungmann were obtained by decomposing graphically the total damping. The validity of some of their interpretations have been discussed elsewhere [19, 20]. Povolo and Molinas [21] have recently studied the HTIF of polycrystalline Zircaloy-4* in detail, for a wide range of frequencies. Two internal friction maxima were observed. The lower temperature peak, also present in pure zirconium, was interpreted in terms of a relaxation mechanism produced by sliding of particle-free grain boundaries. The higher temperature peak was attributed to sliding of boundaries blocked by small precipitates.

It is the purpose of this paper to present new data on the HTIF of polycrystalline zirconium, in particular, on the hysteresis effects observed on the damping spectrum [7, 8]. Furthermore, it will be shown how the hysteresis effects depend on the grain size and that the HTIF of zirconium shows characteristics similar to those of Zircaloy-4 and can be interpreted in terms of similar mechanisms.

2. Experimental procedure

The specimens were prepared from zirconium supplied by Teledyne Wah Chang, Albany. The chemical composition supplied by the manufacturer is given in Table I. The original grain size, as measured according to ASTM E 112 standards, was of the order of 20 μm. Prior to the internal friction measurements, the specimens were annealed at 1023 K in high vacuum, during different times to be specified later, to increase the grain size.

TABLE I Main impurities in zirconium (in ppm)

Al	< 35
C	75
Cr	63
Hf	53
Fe	490
O	1050
Mn	< 25
Ni	< 35
N	45
Si	< 40
Ti	< 25
W	< 25

An automatic pendulum working at intermediate frequencies, of the order of 70 sec^{-1} and in high vacuum, was used for the internal friction measurements in polycrystalline wires with 2 mm diameter. This equipment allows measurements of the damping at constant maximum strain amplitude and the internal friction as a function of temperature is recorded automatically for a specified heating or cooling rate. In this type of pendulum, the internal friction is recorded in terms of the energy required to maintain a given oscillation amplitude. Since this energy is proportional to f^{-2}, where f is the oscillation frequency, the recorded internal friction–temperature curve can be distorted if f changes considerably with temperature. A special feature of the pendulum used is that this effect is corrected automatically so that an undistorted recording of the damping as a function of temperature is obtained. The details of the pendulum are given elsewhere [22].

Since the HTIF of zirconium is amplitude dependent [7, 8, 22] the procedure described in [22] was used to obtain the intrinsic damping, Q_H^{-1}, from the internal friction obtained under the strain distribution given by the torsional oscillations of the automatic pendulum, driven at constant maximum strain amplitude. In fact

$$Q_H^{-1}(\varepsilon) \simeq Q^{-1}(\varepsilon) + \frac{\varepsilon}{4}(\Delta Q^{-1}/\Delta\varepsilon) \qquad (1)$$

*Nominal composition (wt %): Sn (1.41), Fe (0.19), Cr (0.1), Zr (balance).

where $Q^{-1}(\varepsilon)$ is the internal friction measured at a maximum strain amplitude ε and $Q_H^{-1}(\varepsilon)$ gives the intrinsic damping of the material, i.e. the damping that would be obtained under a uniform strain of value ε. $\Delta Q^{-1}(\varepsilon)/\Delta\varepsilon$ can be obtained by making small increments in the strain (or the oscillation amplitude) at different temperatures.

3. Results

Fig. 1 shows the HTIF spectra of two zirconium specimens with an average grain size, l, of 160 μm. Prior to the internal friction experiments the specimens were annealed, in high vacuum, at 1023 K for 250 h, for a grain growth treatment. Curve a was obtained in one of the specimens at a heating rate of 320 K h^{-1}. A maximum temperature of 1243 K was reached, which is above the α/β transition temperature, also indicated in Fig. 1, and the specimen remained for about 0.5 h at this temperature, which was the time needed to realign the optics of the pendulum and to initiate the experiment on cooling. Curve b was obtained during a subsequent cooling at a rate of 80 K h^{-1}.

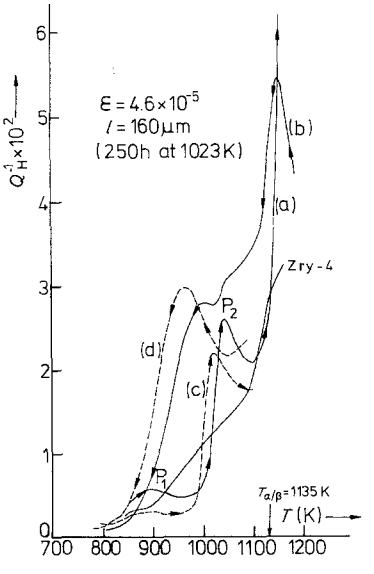

Figure 1 HTIF of polycrystalline zirconium with a grain size of 160 μm. Curve a was obtained in one specimen at a heating rate of 320 K h^{-1} and curve b on cooling at a rate of 80 K h^{-1}. Curves c and d were measured in a similar specimen on heating and on cooling, respectively, at a rate of 80 K h^{-1}. Q_H^{-1} represents the intrinsic damping of the material at a strain amplitude of 4.6 $\times$ 10^{-5}. The HTIF of a Zircaloy-4 specimen is also shown for a comparison.

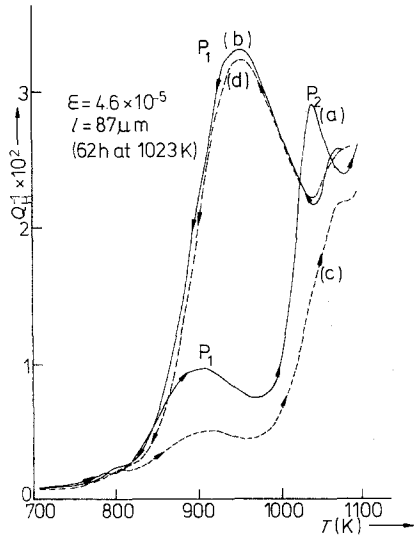

Figure 2 HTIF of polycrystalline zirconium for a grain size of 87 μm, measured at a heating and cooling rate of 80 K h^{-1}. Curves a to d were measured after successive heating and cooling cycles.

The results obtained in the second specimen, at a heating and cooling rate of 80 K h^{-1}, are indicated by curves c and d. This specimen reached a maximum temperature of 1108 K for about 1 h. The HTIF of a Zircaloy-4 wire is also shown in Fig. 1 for comparison. The intrinsic damping plotted against temperature at a strain amplitude $\varepsilon = 4.6 \times 10^{-5}$ is given in Fig. 1. Q_H^{-1} was calculated from the measured curves by using Equation 1 and a strain increment $\Delta\varepsilon = 1.2 \times 10^{-5}$.

Fig. 2 shows the HTIF spectra for a zirconium specimen with an average grain size of 87 μm measured at a heating and cooling rate of 80 K h^{-1}. Prior to the internal friction experiments the specimen was annealed, in high vacuum, at 1023 K for 62 h, for a grain growth treatment. During the first run, described by curve a, the specimen reached a maximum temperature of 1098 K for about 1 h. Curve b was measured during a subsequent cooling, reaching a minimum temperature of 613 K. The specimen was maintained at this temperature for 12 h and a new heating cycle produced curve c; the specimen reached a maximum temperature of 1108 K for about 0.25 h and curve d was obtained during a subsequent cooling.

An inspection of Figs. 1 and 2 reveals that the HTIF spectrum of polycrystalline zirconium consists mainly of two internal friction peaks P_1

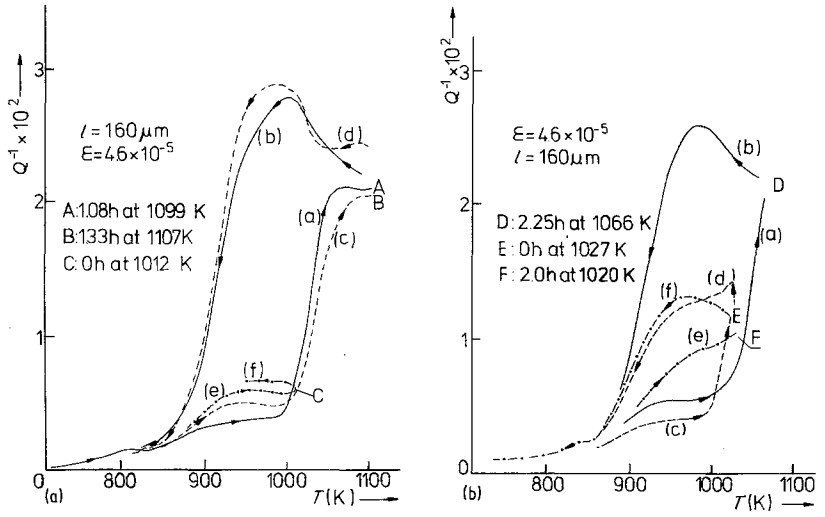

Figure 3 (a) Influence of thermal cycling on the HTIF of the same specimen as for curves c and d of Fig. 1. The curves were obtained at a heating and cooling rate of 80 K h^{-1}. The specimen was maintained at the higher temperatures during the times indicated, before the cooling cycle. (b) HTIF obtained during additional thermal cycling of the specimen used for (a). The specimen was maintained at the higher temperature during the times indicated, before the cooling cycle.

and P_2 and an increasing background, in addition to the maximum due to the α/β transition [23, 24]. Furthermore, both peaks are present when the internal friction is measured on heating but P_1 increases and P_2 disappears during the cooling cycle. Since, as pointed out in Section 1 the damping spectrum of zirconium shows a hysteresis anomaly when the sample is thermally cycled, several experiments were performed to study the influence of the temperature reached during the thermal cycles on the HTIF. It will be shown that the damping can be classified into two types: one similar to curve c of Fig. 1, i.e. a small peak P_1 and a large peak P_2, which will be called c-type damping; another one similar to curve d of Fig. 1, showing only a large peak P_1, which will be called d-type damping. Furthermore, since the amplitude dependence does not change substantially, at least at low strain amplitudes, the general behaviour of the damping–temperature curves, only the measured damping, will be reported. This is to avoid the holding times needed to obtain the intrinsic damping in the way suggested by Equation 1, at the different temperatures. In what follows the maximum strain amplitude used for the measurements will be indicated on each figure.

Figs. 3a and b show the results obtained in the specimen used for curves c and d of Fig. 1. Curve a of Fig. 3a was obtained on heating the specimen to 573 K, maintaining it for 12 h and then raising the temperature at 80 K h^{-1} up to a maximum of 1118 K. The temperature was regulated at 1099 K for 1.08 h and curve b was measured on cooling to 804 K at 80 K h^{-1}. The specimen remained at this temperature for 11 h and curve c was obtained on heating to a maximum temperature of 1115 K at a rate of 80 K h^{-1}. The temperature was regulated at 1107 K for 1.33 h and curve d was obtained during a subsequent cooling, at the same rate, to 813 K. After holding the specimen for 0.4 h at this temperature, curve e was measured on heating to 1012 K at a rate of 80 K h^{-1} and curve f during a subsequent cooling to 948 K at the same rate. The specimen was cooled to 893 K at a rate of 320 K h^{-1} and the temperature was regulated at this value for 10 h. The temperature was decreased further to 790 K at a rate of 320 K h^{-1} and curve a of Fig. 3b was obtained on heating to 1071 K at a rate of 80 K h^{-1}. The temperature was regulated at 1066 K for 2.25 h and curve b of Fig. 3b was measured on cooling to 810 K at a rate of 80 K h^{-1}. After holding the specimen for 12 h at this temperature, a new heating cycle at the same rate to 1027 K leads to curve c; curve d was obtained after an immediate cooling to 805 K at the same rate. Finally, curve e was measured on heating immediately to 1033 K at a rate of 80 K h^{-1} and curve f on cooling at the same rate, after holding the specimen for 2.0 h at 1020 K.

Fig. 4 shows the hysteresis observed in a speci-

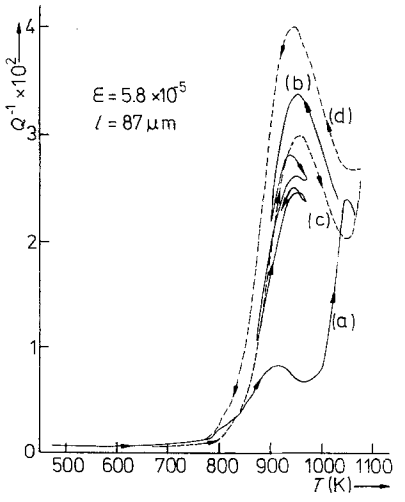

Figure 4 Influence of thermal cycling on the HTIF of a specimen with a grain size of 87 μm. During the last cooling cycle at 320 K h^{-1}, described by curve d, the specimen reached 483 K.

men with a grain size of 87 μm, similar to the one used for Fig. 2. Curve a was obtained on heating, at a rate of 80 K h^{-1}, up to 1074 K and curve b on cooling at the same rate. Several cooling and heating cycles were performed at the same rate, as indicated by the full curves in the same figure. In the last cycle, the specimen is cooled to 723 K, where it is maintained for 15 h. The temperature is decreased again, at 320 K h^{-1}, to 676 K and curve c was obtained during a subsequent heating to 1083 K at 320 K h^{-1}. A cooling cycle at the same rate to 483 K produced curve d. Curve a of Fig. 5a shows the damping spectrum obtained on heating the same specimen from 483 K to 1073 K at a rate of 80 K h^{-1}. Curve b was measured on cooling at the same rate, after holding the specimen for 0.5 h at this temperature. Next, the specimen was subjected to various heating and cooling cycles, at a rate of 80 K h^{-1}, as indicated by the full curves of Fig. 5b. The different curves of this figure have been shifted along the temperature axis to avoid superposition. Curve a is located correctly in temperature, curve b has been shifted by 100 K, curve c by 200 K and curve d by 300 K, to the right with respect to a. The thermal cycling of the specimen has been continued, as shown in Figs. 5c and d, but at a heating rate of 80 K h^{-1} and a cooling rate of 320 K h^{-1}. In Fig. 5c, curve e is located correctly in temperature, but curve f has been displaced by 100 K and curve g by 200 K, to the right with respect to e, to avoid superposition. During the last cooling cycle, given by curve g of Fig. 5c or the beginning of curve h of Fig. 5d, a lower temperature of 637 K was reached. Finally, curve i of Fig. 5d was obtained after turning off the power supply to the furnace of the pendulum.

4. Discussion

As shown in Figs. 1 and 2, c-type HTIF is observed when the measurements are performed on heating and d-type damping is generated on cooling; an additional heating cycle gives c-type damping. As suggested by Ritchie and Sprungmann [7, 8], however, if the specimen is not cooled below a certain critical temperature, T_c, d-type damping is repeated during the heating cycle. Furthermore, according to these authors the critical temperature should be of the order of 723 K.

The thermal cycles performed to establish the presence of a critical temperature, for a specimen with a grain size of 160 μm, have been presented in Figs. 3a and b. The same cycles led us to study the influence of the higher temperature on the subsequent cooling branch. For the different temperatures and times indicated (points A, B, D, E and F) it is seen that a d-type damping is obtained, its intensity being proportional to the temperature. Furthermore, there is no substantial influence of the holding times at the higher temperatures as is shown by cases E and F. The slight difference can be attributed to the inertia of the system in the presence of a fast change from heating to cooling (point E). On the contrary, the higher temperature 1012 K, reached at point C, is not enough to generate a d-type curve on cooling. Referred to the critical temperature, for a specimen with a grain size of 160 μm, three neighbouring values, 813, 810 and 805 K, were mentioned above. In all cases the temperature was obtained after a cooling cycle along a d-type curve. After different holding times (0.4, 12 and 0 h, respectively) a c-type curve was measured. Small differences exist in the intensity of those c-type curves related to the corresponding holding times (the shorter the time, the higher the damping) indicating that time plays a role, although of minor importance, on the phenomenon determining the critical temperature. In summary, it can be stated that the critical temperature for this specimen

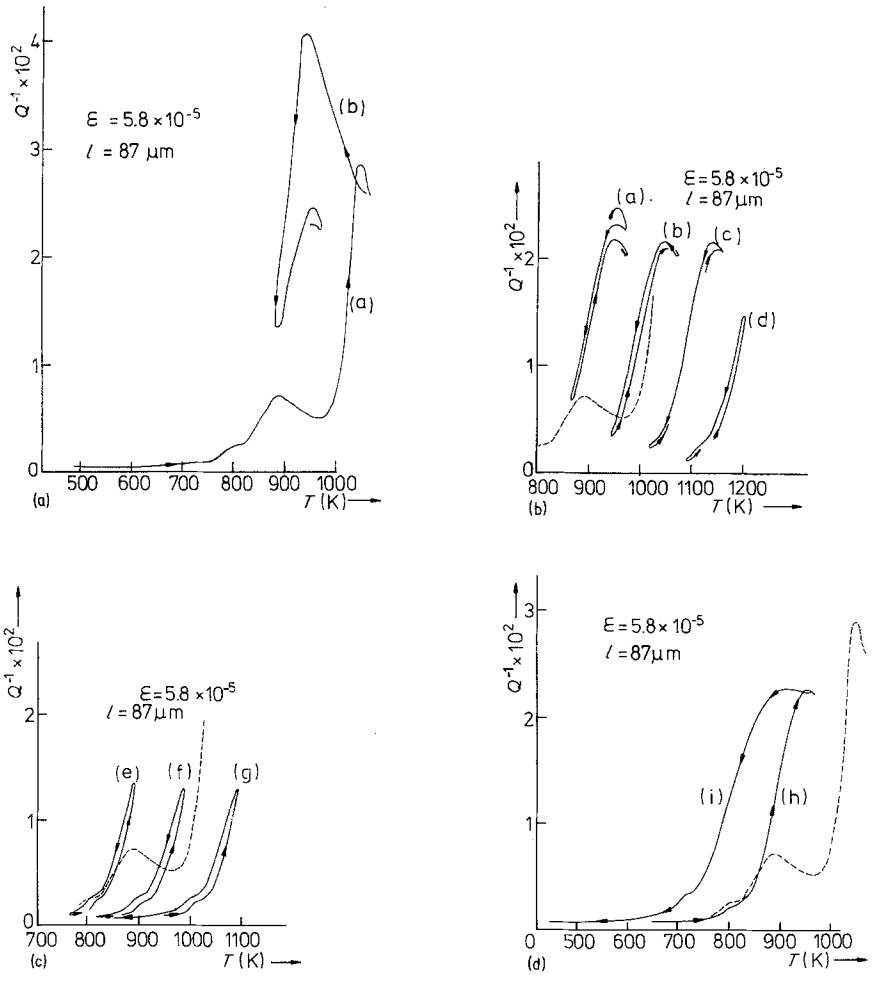

Figure 5 (a) HTIF obtained during additional thermal cycling of the same specimen as for Fig. 4, at a heating and cooling rate of 80 K h^{-1}. (b) HTIF following additional thermal cycling to those shown in (a), at a cooling and heating rate of 80 K h^{-1}. Curve a is located correctly in temperature, but curve b has been shifted by 100 K, curve c by 200 K and curve d by 300 K to the right with respect to curve a, to avoid superposition. The broken curve represents part of curve a of (a). (c) HTIF following additional thermal cycles to those shown in (b), at a heating rate of 80 K h^{-1} and a cooling rate of 320 K h^{-1}. Curve e is located correctly in temperature, but curve f has been shifted by 100 K and curve g by 200 K to the right with respect to curve e, to avoid superposition. A lower temperature of 637 K was reached during the cooling cycle of curve g. The broken curve represents part of curve of (a). (d) HTIF following additional thermal cycles to those shown in (c). The broken curve represents curve a of (a).

(160 μm) is at least of the order of 813 K. Furthermore, it is seen that the above mentioned phenomenon is saturated below 813 K, taking into account that the same c-type curve of low damping (curve c of Fig. 3b and curve a of Fig. 3a) is obtained when the holding time is the same, 12 h, in spite of the great difference between the holding temperatures (810 and 573 K respectively).

The heating cycles used to find the critical temperature for a specimen with a grain size of 87 μm are illustrated in Figs. 4 and 5. During the cycles described in Fig. 4 always d-type damping is produced, except for the first heating cycle from room temperature, described by curve a. During the last cooling cycle, described by curve d, the specimen reached a minimum temperature of 483 K. The next heating cycle, described by curve a of Fig. 5a, produced c-type damping. From these results it can be stated that the critical temperature must be equal to or higher than 483 K. The additional thermal cycles, illustrated in Fig. 5, were performed to establish a more accurate value of the critical temperature.

TABLE II Grain-size dependence of the critical temperature for a transition from d-type to c-type damping

l (μm)	T_c (K)
87	483–637
160	813

During the cycles described by curve b of Fig. 5a and those given in Figs. 5b, c and d only d-type damping was observed. This can be easily established by comparing the full curves of Figs. 5b, c and d with the broken curves of the same figures, which correspond to curve a of Fig. 5a. A further confirmation is given by curve h of Fig. 5d, since only a reduced excursion in temperature was made during the thermal cycles given in Figs. 5b and d. Since the minimum temperature reached during all these cycles was 637 K, i.e. the temperature reached during the cooling cycle of curve g of Fig. 5c, it can be stated that the critical temperature must be located between 483 and 637 K.

The critical temperatures obtained for both specimens are summarized in Table II. It is clear that the critical temperature depends strongly on the grain size.

As reported by Povolo and Molinas [21], two peaks, P_1' and P_2', were also found on the HTIF spectrum of Zircaloy-4. The lowest temperature peak, P_1', was interpreted in terms of a theory, proposed by Sun and Kê [25], of the internal friction produced by relaxation processes occurring in the grain boundaries. This internal friction can be approximately described by [21]

$$Q^{-1} = 0.293\pi(1 - \nu)[\omega\tau/(1 + \omega^2\tau^2)] \quad (2)$$

with

$$\tau = \tau_0 T \exp(\Delta H_b/kT) \quad (3)$$

and

$$\tau_0 = (1 - \nu)\pi kl/4.269\,\mu a\boldsymbol{b}D_{b0} \quad (4)$$

where ν is Poisson's ratio, μ is shear modulus, k is Boltzmann's constant, $\omega = 2\pi f$ is the angular frequency of the applied stress, $\boldsymbol{b}$ is Burgers vector and $a \approx \boldsymbol{b}$ is the average length of a segment of grain boundary mobile dislocations [25], and

$$D_b = D_{b0} \exp(-\Delta H_b/kT) \quad (5)$$

is the diffusion coefficient along grain boundaries. Furthermore, the theoretical peak width at half maximum is given by [21]

$$\Delta(T^{-1}) = (2.199 - \ln T)\,k/\Delta H_b \quad (6)$$

and, since in general $\ln T \ll 2.199$, Equation 6 reduces to

$$\Delta(T^{-1}) = 2.199k/\Delta H_b \quad (7)$$

Equation 7 shows that Equation 2 predicts an internal friction peak slightly narrower than a Debye peak, since in the latter case the peak width at half maximum would be given by [26]

$$\Delta(T^{-1}) = 2.635k/\Delta H_b \quad (8)$$

The same mechanism was proposed for peak P_1, measured on cooling in polycrystalline zirconium [20, 21], since similar values were obtained for the parameters that describe P_1 and P_1'. Peak P_2', obtained in Zircaloy-4 at higher temperatures, was interpreted in [21] as produced by sliding of grain boundaries containing segregated solutes. Furthermore, at least within experimental error, the same value was obtained for the activation enthalpy of P_1, P_1' and P_2', i.e.

$$\Delta H_b = (330 \pm 20)\,\mathrm{kJ\,mol^{-1}} \quad (9)$$

We propose in this paper that peak P_2, measured in zirconium at the higher temperature, is produced by a mechanism similar to that which gave rise to P_2' in Zircaloy-4. In fact, it was shown in [21] that the concentration of impurities, c, needed to saturate the grain boundaries, in a specimen of radius r and length L, is given by

$$c = (dw/\Omega\varrho N_A)\left(\frac{3}{l} - \frac{2}{r} - \frac{2}{L}\right) \quad (10)$$

where d is the thickness of the grain boundary, w is the atomic weight of the solvent atoms, N_A is Avogadro's number, ϱ is the density of the material and Ω is the atomic volume. Since l is much smaller than r and L, on taking $\Omega = b^3$, $d = b$, where b is the lattice parameter, Equation 10 reduces to

$$c \simeq 3w/b^2\varrho N_A l \quad (11)$$

In the case of zirconium and $l = 30\,\mu$m, Equation 11 gives $c = 2.2 \times 10^{-5}$, showing that only a very small amount of impurities are needed to observe a blocking effect of the grain boundaries. Figs. 6a and b show the details of peaks P_1 and P_2, measured on heating, and peak

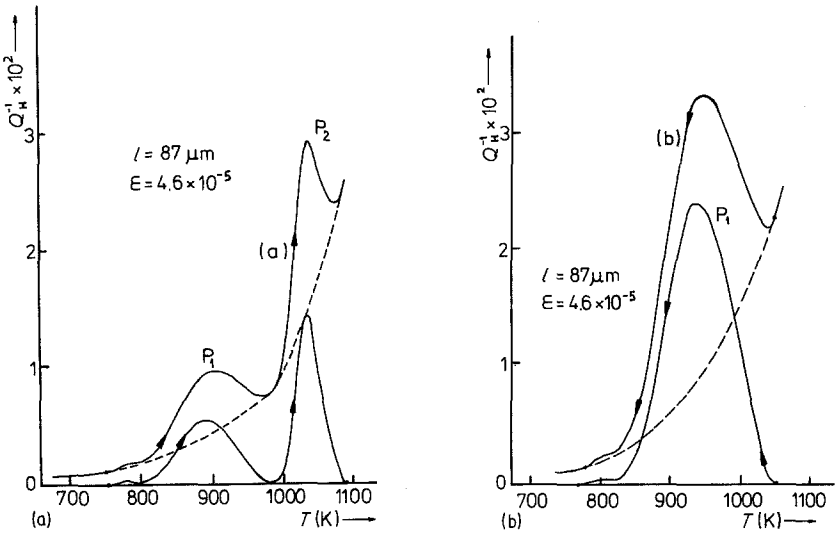

Figure 6 (a) Total intrinsic damping, (a), and high temperature background (HTB), represented by the broken curve, corresponding to curve a of Fig. 2. The two peaks shown are resolved after subtracting out the HTB from the total damping. Data obtained on heating. (b) Total intrinsic damping, (*b*), and HTB, represented by the broken curve, corresponding to curve b of Fig. 2. Peak P_1 is resolved after subtracting out the HTB from the total damping. Data obtained on cooling.

P_1, measured on cooling, in the specimen with a grain size of 87 μm. These curves correspond to the cycles described by curves a and b of Fig. 2, respectively, obtained at a heating or cooling rate of 80 K h^{-1} and were selected due to the fact that both the internal friction peaks and the background are fairly well defined. There are some problems, however, when the background damping is subtracted out from the total damping to obtain the internal friction peaks. In fact, the procedure generally used is to assume that the background damping increases exponentially with the reciprocal of the temperature [20, 27], i.e.

$$Q_{HTB}^{-1} \propto \exp(-\Delta H_{HTB}/kT) \qquad (12)$$

where Q_{HTB}^{-1} is the background damping and ΔH_{HTB} the corresponding activation enthalpy. According to Equation 12, a plot of ln Q_{HTB}^{-1} against $1/T$ should lead to a straight line of slope $\Delta H_{HTB}/k$. A plot of the logarithm of the total damping, given in Figs. 6a and b, against the reciprocal of the temperature is shown in Fig. 7. As shown by curve b of Fig. 7, which corresponds to curve b of Fig. 6b, an approximate straight line, A, can be drawn to define a high

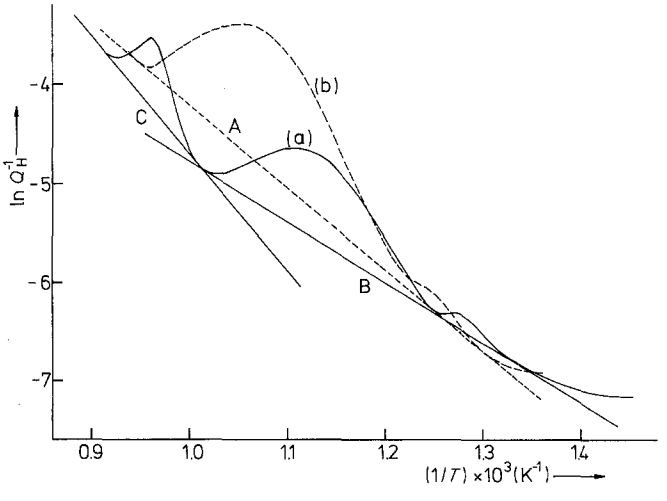

Figure 7 Plot of ln Q_H^{-1} against T^{-1} for the curves of Figs. 6a and b. Straight line, A, represent the HTB of Fig. 6b and straight lines B and C the HTB of Fig. 6a, respectively.

TABLE III Characteristics of peaks P_1 and P_2 shown in Figs. 6a and b. Q_m^{-1} gives the peak height, f_p the frequency at the peak temperature, T_p, and $\Delta(T^{-1})$ the peak width at half maximum, h indicates data obtained on heating and c on cooling, respectively.

Peak	Q_m^{-1} ($\times 10^{-2}$)	f_p (sec^{-1})	T_p (K)	$\Delta(T^{-1})$ (K^{-1})	ΔH_{HTB} ($kJ\,mol^{-1}$)
P_1^h	0.54	70.63	893	1.2×10^{-4}	51
P_2^h	1.4	60.63	1039	3.6×10^{-5}	98
P_1^c	2.4	67.67	938	1.3×10^{-4}	69

temperature background increasing exponentially with the reciprocal of the temperature. The situation is completely different for curve a of Fig. 6a since when this curve is plotted as $\ln Q^{-1}$ against $1/T$ a single straight line cannot be drawn to represent the high temperature background, as shown by curve a of Fig. 7. It is clear that in this case the background damping is not described by Equation 12. In any case and in order to subtract an approximate background two straight lines were assumed, indicated as B and C in Fig. 7.

The background dampings obtained in this way are described by the broken curves of Figs. 6a and b. The internal friction peaks, obtained after subtracting out the HTB from the total damping, are indicated in the same figures. The characteristics of peaks P_1 and P_2 obtained on heating and P_1 measured on cooling, are given in Table III. The small peak at lower temperatures, shown in Figs. 6a and b, is produced by interstitial oxygen [28] and will not be considered in this paper.

The theoretical peak width at half maximum, as given by Equation 7 with ΔH_b given by Equation 9, is

$$\Delta(T^{-1}) = 5.5 \times 10^{-5} K^{-1} \qquad (13)$$

On comparing the value predicted by Equation 13 with the experimental values, reported in Table III, it is seen that peak P_1 is much wider, both during the heating and the cooling cycle. A similar situation was found for peak P_1' in Zircaloy-4 and the possible reasons for a broadening of the experimental peak have been pointed out elsewhere [21]. Furthermore, peak P_2 seems to be narrower than peak P_1 since according to Table III the theoretical and the experimental widths almost coincide. An analogous situation was encountered for peak P_2' in Zircaloy-4 [21] where, in general, peak P_2' is narrower than peak P_1'. It should be pointed out, however, that the data for peak P_2 should be considered with caution since, as shown in Fig. 7, the HTB does not increase exponentially with the reciprocal of temperature. The indetermination in the HTB might lead to a large error in the measured value of $\Delta(T^{-1})$. In addition, it is not clear that peak P_2 can be described by an equation similar to Equation 2, which is valid for particle-free boundaries.

If the model used to describe both peaks is correct, i.e. peak P_1 as produced by particle-free boundaries (orthodox grain boundary peak) and P_2 as produced by particle-bearing boundaries, an estimation of the interplanar spacing between particles can be performed. In fact, the broadening of peak P_1 is due to the fact that the actual specimen has a distribution of grain sizes and the theory assumes that all the grains have the same dimensions. On assuming that the distribution is normal in $\ln l$ (lognormal distribution), the procedure suggested by Nowick and Berry [29] can be used to obtain an estimation of the influence of the grain-size distribution on the relaxation strength. In fact [21]:

$$r_2(\beta) \simeq [(\Delta H_b/k)\,\Delta(T^{-1}) + \ln T]/2.635 \simeq (\Delta H_b/2.635k)\,\Delta(T^{-1}) \qquad (14)$$

and

$$Q_m^{-1} = 2 f_2(0, \beta)[\Delta_j/(2 + \Delta_j)] \qquad (15)$$

where $\Delta(T^{-1})$ is the measured width and $r_2(\beta)$ and $f_2(0, \beta)$ are functions tabulated in [29] as a function of β. β is a parameter that measures the width of the Gaussian distribution ($\beta = 0$ means a single relaxation time) and Δ_j is the relaxation strength, i.e. twice the height of the peak corresponding to a single relaxation time equal to the average value. Equation 14 can be used to obtain $r_2(\beta)$ from the measured value of $\Delta(T^{-1})$ for peak P_1, measured on cooling, given in Table III. Once $r_2(\beta)$ is known, β can be obtained from the tables of $r_2(\beta)$ against β given in [29]. Furthermore, Δ_j can be obtained by means of Equation 15, on taking the measured value for Q_m^{-1}, given in Table III, and $f_2(0, \beta)$

obtained from the tabulated values as a function of β given in [29]. This procedure applied to peak P_1, shown in Fig. 6b, leads to

$$\Delta_j(P_1^c) = 9.1 \times 10^{-2} \quad (16)$$

For peak P_2 of Fig. 6b, $\beta \simeq 0$, then

$$2Q_m^{-1} = \Delta_j(P_2^h) = 2.8 \times 10^{-2} \quad (17)$$

According to Mori *et al.* [30] the particles in the boundaries reduce the relaxation strength in the factor $(1 + \pi lr/\lambda^2)$, where λ is the interparticle spacing and r is the average radius of the blocking particles. Then

$$\Delta_j(P_2^h) = \Delta_j(P_1^c)/(1 + \pi lr/\lambda^2) \quad (18)$$

which, on taking into account Equations 16 and 17, with $l = 87\,\mu m$ leads to

$$r/\lambda^2 = 0.84 \times 10^4\,m^{-1} \quad (19)$$

If r is of the order of the limit of resolution of an electron microscope, i.e. of the order of $10b$, where $b = 3.23 \times 10^{-10}$ m is the lattice parameter of zirconium, Equation 19 leads to

$$\lambda = 1940b \quad (20)$$

Even if this value is very approximate does not seem unreasonable. Furthermore, an estimation of the interparticle spacing segregated at the grain boundaries in Zircaloy-4, obtained by combining the parameters for peak P_1' with those for peak P_2' gave $\lambda = 70b$ [21]. The model described by Equation 2 predicts an internal friction maximum

$$Q_m^{-1} = 0.293\pi(1 - \nu)/2 \quad (21)$$

which, for $\nu = 0.3$ gives

$$Q_m^{-1} = 0.3 \quad (22)$$

independently from the grain size. Δ_j for peak P_1 measured on cooling (see Equation 16) is not too far from twice the value given by Equation 22. A more detailed model, taking into account the actual distribution of the grain sizes would lead probably to a grain size dependence of Q_m^{-1}, since several simplifying assumptions are used to obtain Equation 21 and Equations 16 and 17.

Some comments should be made to the measurements of the grain size dependence of the HTIF of zirconium, reported by Bungardt and Preisendanz [24]. These data have been considered by Gleiter and Chalmers [2] as an example of the grain size dependence of the internal friction produced by grain boundary sliding. In fact, by using a torsion pendulum, Bungardt and Preisendanz measured the HTIF of zirconium in specimens with grain sizes ranging from about 68 μm to above 200 μm. All the measurements were performed on heating at a rate of 120 K h^{-1} and the grain size was changed by making different thermal treatments, including heating well above the α/β transition temperature. Only one internal friction peak was observed in the temperature region between about 623 and 993 K, which decreased continuously on decreasing the grain size. An internal friction maximum $Q_m^{-1} = 2.3 \times 10^{-2}$ was obtained for $l = 68\,\mu m$ and $Q_m^{-1} = 2 \times 10^{-3}$ for $l = 200\,\mu m$; no peak was detected for $l > 200\,\mu m$. It is clear that these results should be considered with caution for two reasons: first, more uniform grains are obtained, with respect to specimens subjected to the α/β transition, when the treatments are performed in the α-phase for a long time. The different grain-size distributions will affect the HTIF, as can be seen on comparing curves b and d of Fig. 1. Secondly, the hysteresis effects present on the HTIF of zirconium might lead to wrong conclusions about the grain-size dependence of the internal friction. In fact, a completely different HTIF spectrum is obtained when the measurements are performed on cooling, where only the orthodox grain boundary peak is present. On comparing Figs. 1 and 2, for example, it is seen that during the heating cycle, P_1 is lower for the specimen with larger grains. On cooling, however, peak P_1 does not differ substantially in magnitude for the two specimens. Furthermore, a maximum of the order of 2.5×10^{-2} was also observed at lower frequencies (of the order of 1 sec^{-1}) in a zirconium specimen with an average grain size of 40 μm, during measurements performed on cooling [20].

Ogino and Amano [31] have observed a large internal friction peak in aluminium and very dilute Al–Fe alloys, in specimens with "bamboo" structure and for measurements performed on cooling. According to these authors, the occurrence of this peak may be qualitatively accounted for by a mechanism of grain boundary sliding controlled by grain boundary irregularities, such as grain boundary ledges. The segregated impurities will also affect grain boundary sliding.

It might be possible that the characteristics observed on the HTIF spectra of zirconium and Zircaloy-4 are more general and can be present, in more or less extent, in other metals and alloys. Unfortunately, no detailed internal friction studies have been reported for other systems.

The hysteresis effects observed on the HTIF of zirconium, shown in Figs. 1 to 5, and to a lesser extent in Zircaloy-4, can be explained, at least qualitatively, by the model used to interpret peaks P_1 and P_2. In fact, when part of the grain boundaries is blocked by particles both peaks are observed (c-type damping), as shown for example by curve a of Fig. 6a. If a high enough temperature is reached during the heating cycle the diffusivity of the impurities is very high and the boundaries are free from the blocking particles. Only d-type damping will be observed on a subsequent cooling, i.e. only peak P_1 will be present, as shown for example by curve b of Fig. 6b. Furthermore, as shown by the cycles illustrated by Fig. 4, it is clear that the segregation of the impurities to the grain boundaries will occur continuously on cooling and P_1 is reduced as P_2 develops. The critical temperature is only an indication that full segregation has occurred. In addition, when the maximum temperature reached during the heating cycle is not high enough the same type of damping will be repeated during a subsequent cooling, as illustrated by curves a and f of Fig. 3a.

The grain size dependence of the critical temperature can be explained by the fact that, as suggested by Equation 11, more impurities are needed at the grain boundaries as the grain size decreases. Since more impurities are segregated as the temperature decreases, the critical temperature will decrease on decreasing the grain size. A detailed model of the interaction of the impurities with the grain boundaries is needed to be able to make a quantitative estimation of the hysteresis effects. Furthermore, the models used to describe the internal friction produced by grain boundary sliding are based on a continuous model description of the grain boundaries, which is clearly an oversimplification.

As pointed out before, according to Ritchie and Sprungmann [7, 8] the critical temperature should be of the order of 723 K, since this is the temperature at which oxygen interstitials become appreciably mobile in the lattice. In fact, the model used by these authors to explain the hysteresis phenomenon in super-annealed specimens is based on dislocation segments trapped by impurities clouds (oxygen). On heating from below about 723 K, very little internal friction is observed because the dislocation segments are trapped in heavily pinned configurations or impurity clouds. Above about 873 K, transverse drag becomes possible and each segment sweeps out a relatively clean area of lattice. This, in turn, allows all of the mechanisms involving relatively long pin-free lengths to become operative. The relaxation peaks corresponding to these mechanisms can then be observed either on heating or cooling provided that the temperature does not fall below about 723 K, where the segments become repinned and the pinning cloud re-develops. In addition, according to these authors, a similar reasoning also explains the results observed on the single-crystal samples. In summary, according to Ritchie and Sprungmann, the HTIF spectrum of zirconium is explained mainly through processes not confined to grain boundaries, i.e. by thermally assisted unpinning and core redistribution phenomena occurring on dislocations within the grains. The super-annealed condition of large grains must represent an enormous decrease in the overall density of dislocations.

As shown in this paper, the critical temperature depends on the grain size and, as indicated in Table III, it is well below 723 K for a grain size of 87 μm. This is very difficult to understand in the context of the model proposed by Ritchie and Sprungmann. Furthermore, it is not easy to accept that the dislocation density changes drastically between a thermal treatment of 62 h at 1023 K, as for the specimen of Fig. 2 and 250 h at the same temperature, as for the specimen of Fig. 1. In addition, according to Ritchie and Sprungmann the hysteresis effects are observed only when special treatments are given to the specimens, as the one indicated as "vibration conditioning". As shown in this paper, however, no special treatments are needed to observe the hysteresis effects, which are also present in Zircaloy-4. It is clear that the model presented in this paper, i.e. segregation of impurities to grain boundaries seems to be more acceptable. It is difficult to establish, with the available information, the kind of impurities that are interacting with the grain boundaries. Since similar effects were observed in Zircaloy-4

it might be possible that interstitial impurities, such as oxygen, are responsible for the hysteresis effects.

Finally, as shown in Table III, the apparent activation enthalpy for the high temperature background varies with temperature, when the measurements are performed on heating. As shown elsewhere [20] no correlation was found between ΔH_{HTB} and the grain size for zirconium. A different situation was encountered for Zircaloy-4 where ΔH_{HTB} decreased continuously with the grain size.

5. Conclusions

Two internal friction maxima are present on the HTIF of annealed polycrystalline zirconium, when the measurements are performed on heating. After reaching a high enough temperature the peak occurring at the higher temperature disappears during the cooling cycle. If the temperature is not decreased below a certain value (critical temperature) only the lower temperature peak will be observed during a subsequent heating cycle. The critical temperature is strongly dependent on the grain size, decreasing as the grain size is reduced.

Finally, both the hysteresis effects and the two internal friction maxima can be explained by a relaxation mechanism associated with grain boundary sliding and segregation of impurities to the grain boundaries. The lower temperature peak is produced by sliding of the particle-free boundaries and the high temperature peak by sliding of the particle-bearing boundaries.

Acknowledgements

This work was supported in part by the German–Argentine Cooperation Agreement in Scientific research and Technological Development, by the CIC and the "Proyecto Multinacional de Tecnología de Materiales" OAS-CNEA.

References

1. T. S. KÊ, *Phys. Rev.* **71** (1947) 533.
2. H. GLEITER and B. CHALMERS, High-Angle Grain Boundaries, in "Progress in Materials Science", Vol. 16 (Pergamon Press, Oxford, 1972).
3. C. C. SMITH and G. M. LEAK, Proceedings of the 5th International Conference on Internal Friction and Ultrasonic Attenuation in Solids, Vol. II, edited by D. Lenz and K. Lücke (Springer-Verlag, Berlin, 1975) p. 383.
4. C. C. SMITH and G. M. LEAK, *Il Nuovo Cimento* **33B** (1976) 388.
5. C. ESNOUF and G. FANTOZZI, *J. Phys.* **42** (1981) C5-445.
6. A. RIVIERE, J. P. AMIRAULT and J. WOIRGARD, *Il Nuovo Cimento* **33B** (1976) 398.
7. I. G. RITCHIE and K. W. SPRUNGMANN, Atomic Energy of Canada Ltd, Rep., AECL-6810 (1981).
8. *Idem, J. Phys.* **42** (1981) C5-427.
9. A. RIVIERE, J. P. AMIRAULT and J. WOIRGARD, *ibid.* **42** (1981) C5-439.
10. E. BONETTI, E. EVANGELISTA, P. GONDI and R. TOGNATO, *Il Nuovo Cimento* **33B** (1976) 408.
11. P. GONDI, R. TOGNATO and E. EVANGELISTA, *Phys. Status Solidi (a)* **33** (1976) 579.
12. E. BONETTI, E. EVANGELISTA, P. GONDI and R. TOGNATO, *ibid.* **39** (1977) 661.
13. E. BONETTI, L. CASTELLANI, E. EVANGELISTA and P. GONDI, *J. Phys.* **42** (1981) C5-433.
14. *Idem, Phys. Status Solidi (a)* **63** (1981) 645.
15. T. S. KÊ, *J. Phys.* **42** (1981) C5-421.
16. J. L. GACOUGNOLLE, S. SARRAZIN and J. De FOUQUET, *ibid.* **32** (1971) C2-21.
17. *Idem,* Proceedings of the 5th International Conference on Internal Friction and Ultrasonic Attenuation in Solids, Vol. I, edited by D. Lenz and K. Lücke (Springer-Verlag, Berlin, 1975) p. 343
18. J. De FOUQUET, J. WOIRGARD, J. L. GACOUGNOLLE and A. RIVIERE, *J. Phys.* **36** (1975) C4-291.
19. F. POVOLO, *Scripta Metall.* **16** (1982) 885.
20. F. POVOLO and B. J. MOLINAS, *J. Nucl. Mater.* **114** (1983) 85.
21. *Idem, J. Mater. Sci.* to be published.
22. F. POVOLO, A. F. ARMAS and B. J. MOLINAS, *J. Phys. E* **17** (1984) 121.
23. W. J. BRATINA and W. C. WINEGARD, *Trans. AIME* **206** (1956) 186.
24. K. BUNGARDT and H. PREISENDANZ, *Z. Metallkde* **51** (1960) 280.
25. Z. Q. SUN and T. S. KÊ, *J. Phys.* **42** (1981) C5-451.
26. A. S. NOWICK and B. S. BERRY, "Anelastic Relaxation in Crystalline Solids" (Academic Press, New York, 1972).
27. F. POVOLO and B. J. MOLINAS, in "Strength of Metals and Alloys", Vol. 1, edited by R. C. Gifkings (Pergamon Press, Oxford, 1983) p. 8.
28. I. G. RITCHIE and A. ATRENS, *J. Nucl. Mater.* **67** (1977) 254.
29. A. S. NOWICK and B. S. BERRY, *IBM J.* **5** (1961) 297.
30. T. MORI, M. KODA, R. MONZEN and T. MURA, *Acta Metall.* **31** (1983) 275.
31. Y. OGINO and Y. AMANO, *Trans. J. Inst. Metals* **20** (1979) 81.

Received 14 September
and accepted 22 November 1984